**Growth of polyaromatic molecules via ion-molecule reactions: an experimental and theoretical mechanistic study .**

# UNIVERSITÀ DEGLI STUDI DI TORINO

# Growth of polyaromatic molecules via ion-molecule reactions: an experimental and theoretical mechanistic study

Daniela Ascenzi,[1,a)] Julia Aysina,[1] Paolo Tosi,[1] Andrea Maranzana,[2] and Glauco Tonachini[2,a)]

[1] *Dipartimento di Fisica, Università di Trento, Via Sommarive 14, I-38123 Povo, Trento, Italy*
[2] *Dipartimento di Chimica Generale e Chimica Organica, Università di Torino, Corso Massimo D'Azeglio 48, I-10125, Torino, Italy*

**Abstract.** The reactivity of naphthyl cations with benzene is investigated in a joint experimental and theoretical approach. Experiments are performed by using guided ion beam tandem mass spectrometers equipped with electron impact or atmospheric pressure chemical ion sources to generate $C_{10}H_7^+$ with different amounts of internal excitation. Under single collision conditions, C-C coupling reactions leading to hydrocarbon growth are observed. The most abundant ionic products are $C_{16}H_{13}^+$, $C_{16}H_n^+$ (with n=10-12) and $C_{15}H_{10}^+$. From pressure-dependent measurements absolute cross sections of 1.0±0.3 $Å^2$ and 2±0.6 $Å^2$ (at a collision energy of about 0.2 eV in the center of mass frame) are derived for channels leading to the formation of $C_{16}H_{12}^+$ and $C_{15}H_{10}^+$ ions, respectively. From cross section values a phenomenological total rate constant $k$ = (5.8±1.9)×$10^{-11}$ $cm^3 \cdot s^{-1}$ at an average collision energy of about 0.27 eV can be estimated for the process $C_{10}H_7^+$+ $C_6H_6 \rightarrow$ all products. The energy behaviour of the reactive cross sections, as well as further experiments performed using partial isotopic labelling of reagents, support the idea that the reaction proceeds via a long lived association product, presumably the covalently bound protonated phenylnaphthalene, from which lighter species are generated by elimination of neutral fragments (H, $H_2$, $CH_3$). A major signal relevant to the fragmentation of the initial adduct $C_{16}H_{13}^+$ belongs to $C_{15}H_{10}^+$. Since it is not obvious how $CH_3$ loss from $C_{16}H_{13}^+$ can take place to form the $C_{15}H_{10}^+$ radical cation, a theoretical investigation focuses on possible unimolecular transformations apt to produce it. Naphthylium can act as an electrophile and add to the π system of benzene, leading to a barrierless formation of the ionic adduct with an exothermicity of about 53 $kcal \cdot mol^{-1}$.

a) Authors to whom correspondence should be addressed. Electronic addresses: ascenzi@science.unitn.it and glauco.tonachini@unito.it

From this structure, an intramolecular electrophilic addition followed by H shifts and ring opening steps leads to an overall exothermic loss (-7.1 kcal·mol$^{-1}$ with respect to reagents) of the methyl radical from that part of the system which comes from benzene. Methyl loss can take place also from the "naphthyl" part, though via an endoergic route. Experimental and theoretical results show that an ionic route is viable for the growth of polycyclic aromatic species by association of smaller building blocks (naphthyl and phenyl rings) and this may be of particular relevance for understanding the formation of large molecules in ionized gases.

KEYWORDS: atmospheric chemistry, ionization, ion-molecule reactions, mass spectrometry, PAH, planetary ionosphere, polycyclic aromatic hydrocarbon, Titan

## 1. Introduction

Polycyclic aromatic hydrocarbons (PAHs) have been observed in quite different gaseous environments, such as combustion systems or the interstellar medium.[1] Thus understanding how these ubiquitous molecules are formed has become an increasingly important research topic in the last few years. While great progress has been made in the knowledge of synthetic mechanisms based on radical and neutral reactions,[2] much less is known about ionic routes to the synthesis of PAHs. It is worth noting that ionic reactions are not restricted to “obvious” environments (gaseous discharges, plasmas, planetary ionospheres…), but they also occur in unexpected situations, such as hydrocarbon flames [3,4] or the exhaust of aircraft engines.[5] The formation of ionized naphthalene from the reaction of benzene radical cations with diacetylene was described and proposed almost 20 twenty years ago as a general model for the growth of PAHs by ion-molecule reactions.[6] More recently, the formation of benzene ions within ionized acetylene clusters has been reported.[7] In turn, benzene ions can catalyze the polymerization of acetylene molecules and possibly their conversion into naphthalene-type ions.[8] In addition, the reactions of benzene radical cation with pyridine and of pyridine radical cation with

benzene have been recently shown [9] to afford a covalently bound adduct via a C-N bond forming process. This is indeed quite interesting because it extends the synthetic growth mechanisms to N-containing species.

Growth routes for unsaturated hydrocarbons based on the reactivity of doubly charged ions have been also explored [10] with special reference to the requirement of new laboratory data for modelling the Titan's atmosphere, given the information now available from the Cassini-Huygens mission. An unexpected result from the Cassini flybys of Titan was the discovery of benzene at high altitude[11] and the presence of large mass (over 100 amu) positive and negative ions in significant amounts in Titan's ionosphere below 1200 km.[12] Among the possible structures of such large mass molecules fused-ring polycyclic aromatic hydrocarbon compounds (*e.g.* naphthalene and anthracene, but also nitrile aromatic polymers[13]) have been proposed, as well as fullerenes[14] and polyphenyls[15]. All such structures are compatible with Cassini detections and such heavy particles have been proposed to be the precursors to the haze particles which form the optically thick haze layer lower in Titan's atmosphere.[16] In spite of several laboratory investigations, new experimental and theoretical data are still required to provide a quantitative comparison between the *in situ* observations of the Cassini orbiter and the proposed models.[16]

In the recent past we have explored ionic mechanisms for the growth of larger molecules starting from phenyl cations.[17,18] In the present paper we report on new measurements about the reactivity of the naphthyl cation $C_{10}H_7^+$ with benzene $C_6H_6$. We have observed the growth of hydrocarbon ions up to $C_{16}H_{13}^+$ species, via C-C bond forming reactions. Experimental data are discussed in light of DFT theoretical calculations.

## 2. Experimental methods

The reaction of naphthyl cation $C_{10}H_7^+$ with benzene (both $C_6H_6$ and $C_6D_6$) has been investigated by using both a home-built guided-ion beam apparatus (GIB-MS), and an Applied Biosystem Triple Quadrupole mass spectrometer API 3000$^{TM}$ LC/MS/MS equipped with an Atmospheric Pressure Chemical Ion (APCI) source (in the following indicated as APCI-TQ-MS). The guided ion beam set-up is a tandem mass spectrometer with an $O_1Q_1O_2Q_2$ configuration (Q stands for quadrupole and O for octopole) as described elsewhere.[17,19,20] Naphthyl ions are generated by dissociative electron ionization (EI) of 1-chloronaphthalene, and are mass selected by quadrupole $Q_1$ before being injected into octopole $O_2$, which is surrounded by the scattering cell filled with benzene at the desired pressure (monitored by a spinning rotor gauge MKS SRG2). The kinetic energy of the projectile ion beam in the laboratory frame, which determines the collision energy, can be varied from practically 0 to several tens of eV by changing the DC bias potential of $O_2$. Lab frame collision energies, $E_{LAB}$, are converted to the corresponding values in the center-of-mass frame, $E_{CM}$, via the formula $E_{CM} = m/(M+m) \cdot E_{LAB}$, where $m$ and $M$ stand for the mass of the neutral target and the ionic projectile, respectively. Product ions are mass analyzed by $Q_2$ and detected by an electron multiplier. The ratio between the measured signal intensities of product and reactant ions is proportional to the effective integral cross section and its absolute value can be measured, in a beam-cell experiment, according to the Lambert-Beer law. For low pressures of neutral target (thin target limit) the Lambert-Beer law can be approximated as: $I_P/I_0 = \sigma_P \cdot n \cdot l_{eff}$, where $I_P$ and $I_0$ are the intensity of products P and reagent ions, respectively (with $I_P << I_0$), $n$ is the neutral gas density in the collision cell, and $l_{eff}$ is the effective lenght of the collision cell, equal to $12.0 \pm 0.6$ cm in our case.[17] By measuring the slope of the plot of $I_P/I_0$ as a function of the neutral gas density (at sufficiently low densities to ensure single collision regime), we can obtain effective reactive cross sections $\sigma_P$ for each of the reaction channels. In such type of measurements, the

accuracy is limited by uncertainties in the measurement of the gas pressure and by error propagation due to the calibration procedure necessary to establish the value of $l_{eff}$. We estimate that absolute cross section values are accurate within ±30%.

In the experiments performed with the APCI-TQ-MS, reactant ions are generated from 1-chloronaphthalene as neutral precursor in an Atmospheric Pressure Chemical Ionization – Heated Nebulizer Source (by AB Sciex). The precursor is injected (via a micrometric syringe pump, injection flow in the range 1-10 μl/min) as solution in methanol with a concentration 0.1 M using high purity $N_2$ (obtained by the boil-off from a liquid nitrogen dewar) both as nebulizer and curtain gas. Measurements are performed with the source heated at 400 ℃ and the best set of operating cond itions to optimize the production of $C_{10}H_7^+$ ions are found to be the followings: nebulizer gas pressure 45 psi, auxiliary gas 11 psi, curtain gas 7 psi, declustering potential 95 V, current of the corona discharge needle 2.5 μA, focussing potential 230 V, entrance potential 5 V. The advantage of producing naphthyl cations via the corona discharge of the APCI source rather than by EI in the GIB-MS ion source relies in the lower internal excitation of the primary ion, as demonstrated by the absence of unimolecular fragmentation into $C_7H_7^+$ (*m/z* 77) during the flight from the source to the detector. Ion-molecule reactions of $C_{10}H_7^+$ with $C_6H_6$ and $C_6D_6$ are carried out by injecting benzene into the collision cell quadrupole, at a pressure in the range $10^{-5}$-$10^{-3}$ mbar. To admit vapours or gases other then $N_2$ into the CAD cell of the APCI-TQ-MS instrument, the gas injection line has been modified as described in details in our previous paper.[18]

## 3. Theoretical methods

Stationary points on the energy hypersurface are determined by gradient procedures,[21] within Density Functional Theory (DFT)[22] and making use of the M06-2X

functional.[23] Dunning's cc–pv*TZ* basis set[24] is used in the DFT optimizations and subsequent vibrational analyses and thermochemistry assessments. Single point energy evaluation are also performed at cc–pv*QZ* to exploit the two-term extrapolation formula by Halkier *et al*.[25] that allows an estimate of the complete basis set (CBS) limit. The relative energies are corrected by the cc–pv*TZ* zero point vibrational energy ($\Delta E_{ZPE}$) and reported in the Schemes. Energetics is reported in kcal·mol$^{-1}$ throughout the paper. All calculations are carried out by using the GAUSSIAN 09 system of programs.[26]

## 4. Results and discussion

### 4.1 Experimental results

The reaction of naphthylium ions with benzene leads to the growth of larger hydrocarbon species via C-C bond forming reactions. In the case of benzene-$h_6$, the occurrence of such reactions is evidenced by the detection of ions $C_{16}H_n^+$ with n=13-10 (*m/z* 202-205), $C_{15}H_n^+$ with n=9-10 (*m/z* 189 e 190), $C_{14}H_n^+$ with n=9-11 (*m/z* 177-179), $C_{13}H_9^+$ (*m/z* 165), and $C_{12}H_{11}^+$ (*m/z* 155) in the mass spectrum recorded at low collision energy using the GIB set-up equipped with the EI source (see typical mass spectra reported in Figure 1 at two different pressures of benzene-$h_6$ in the scattering cell). In conjunction with the mass shifts observed upon using benzene-$d_6$ as reactant (data not shown), the generation of such ions is attributed to the occurrence of the following reactions:

$$C_{10}H_7^+ + C_6H_6 \rightarrow C_{16}H_{13}^+ \text{ (}m/z\text{ 205)} \quad (1)$$

$$\rightarrow C_{16}H_{12}^+ \text{ (}m/z\text{ 204)} + H \quad (2)$$

$$\rightarrow C_{16}H_{11}^+ \text{ (}m/z\text{ 203)} + H_2 \quad (3)$$

$$\rightarrow C_{16}H_{10}^+ \text{ (}m/z\text{ 202)} + H+H_2 \quad (4)$$

$$\rightarrow C_{15}H_{10}^+ \text{ (}m/z\text{ 190)} + CH_3 \quad (5)$$

$$\rightarrow C_{15}H_9^+ \text{ (}m/z\text{ 189)} + CH_3+H \quad (6)$$

$\rightarrow C_{14}H_{10}^{+}$ (*m/z* 178) + $C_2H_3$ (7)

$\rightarrow C_{13}H_9^{+}$ (*m/z* 165) + $C_3H_4$ (8)

$\rightarrow C_{12}H_{11}^{+}$ (*m/z* 155) + $C_4H_2$ (9)

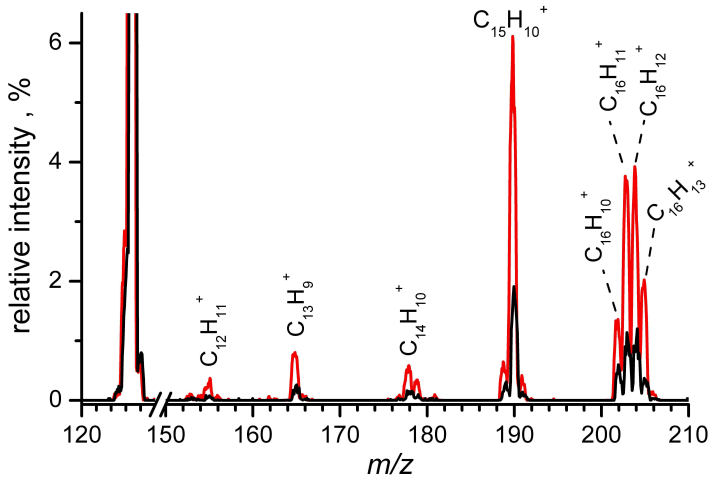


**Figure 1:** MS spectrum of ionic products from the reaction of mass-selected $C_{10}H_7^+$ ions with $C_6H_6$ recorded in the GIB-MS set up at a collision energy $E_{CM}$ ~ 0.2 eV in the center of mass frame and with $1.8\times10^{-4}$ mbar (black) and $8\times10^{-4}$ mbar (red) of benzene in the reaction cell. The signal intensity of the parent ion (100%) is off-scale.

The branching ratios (or relative yields) of product ions at two different pressures are shown in columns *(a)* and *(b)* of Table 1. At low benzene pressure the formation of the $C_{16}H_{13}^+$ ion is indeed observed experimentally though in a rather low relative yield. The latter is however increasing with the pressure (from 5% to 9%, corresponding to an increase of the pressure from $1.8\times10^{-4}$ mbar to $8\times10^{-4}$ mbar, see Table 1), indicating that multiple collisions allow an efficient dissipation of the energy liberated upon association, thus providing stabilization of the initially excited addition complex, and formation of a long-lived species, most likely the covalently bound protonated phenylnaphthalene, formed via electrophilic addition of naphthyl cation to the benzene ring.

As well as on specific pressures and collision energy conditions, the relative ionic yields of the various channels are found to be dependent on the ionization method used to generate the $C_{10}H_7^+$ primary ions. Values referring to the use of the APCI-TQ-MS are reported in column *(c)* of Table 1, while a typical mass spectrum is shown in Figure 2. The most striking difference between the ion yields measured by using two different methods for the generation of naphthyl cations (namely EI ionization in GIB-MS and APCI ionization

in TQ-MS) is observed for the association product $C_{16}H_{13}^+$: in the case of EI generation (see Figure 1 and Table 1) the yield of $C_{16}H_{13}^+$ amounts to about 9% (at a pressure of benzene ~$8\times10^{-4}$ mbar), the main product being $C_{15}H_{10}^+$ produced according to reaction (5) above. Conversely, for APCI generation (see Figure 2 and Table 1) the association product predominates with a yield of about 78% (at a similar value of benzene pressure).

| ***m/z*** | **Ion** | *Branching ratios (%)* | | |
|---|---|---|---|---|
| | | *(a)* | *(b)* | *(c)* |
| Others | | 0 | 0 | 1.0 |
| 153 e 155 | $C_{12}H_n^+$ n=9,11 | 2 | 3 | 0.1 |
| 165 e 166 | $C_{13}H_n^+$ n=9,10 | 4 | 5 | 0.3 |
| 177-181 | $C_{14}H_n^+$ n=9-13 | 4 | 5 | 0.4 |
| 189-191 | $C_{15}H_n^+$ n=9-10 | 38 | 34 | 5.5 |
| 202 | $C_{16}H_{10}^+$ | 9 | 6 | 1.1 |
| 203 | $C_{16}H_{11}^+$ | 19 | 20 | 7.2 |
| 204 | $C_{16}H_{12}^+$ | 19 | 18 | 6.1 |
| 205 | $C_{16}H_{13}^+$ | 5 | 9 | 78.3 |
| Total | | 100 | 100 | 100 |

**Table 1:** Branching ratios for formation of the various product channels observed upon reaction of $C_{10}H_7^+$ with benzene-$h_6$ at the following conditions: *(a)* GIB-MS, benzene pressure $1.8\times10^{-4}$ mbar, *(b)* GIB-MS, benzene pressure $8\times10^{-4}$ mbar, *(c)* APCI-MS, benzene pressure $9.5\times10^{-4}$ mbar. Errors on the branching ratios are about 10%.

The difference is attributed to the internal excitation of the $C_{10}H_7^+$ reacting ion, which is expected to reduce the lifetime of the intermediate complex and the probability for its stabilization into a long-lived species. The EI source of the GIB-MS apparatus operates at low pressure and therefore collisional cooling of the nascent ions is ineffective. On the contrary, $C_{10}H_7^+$ ions produced into the APCI source can dissipate the excess of internal energy by collisions with $N_2$ at atmospheric pressure prior to reaction with benzene.

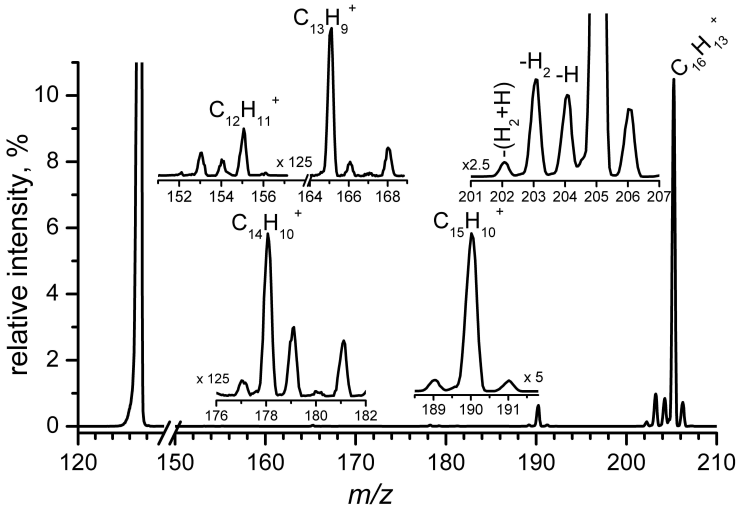


**Figure 2:** MS spectrum of ionic products from the reaction of mass-selected $C_{10}H_7^+$ ions with $C_6H_6$ recorded in the APCI-TQ-MS set up at a collision energy $E_{CM}$ ~ 1 eV in the center of mass frame and with ~$9.5\times10^{-4}$ mbar of benzene in the reaction cell. The signal intensity of the parent ion (100%) is off-scale.

The ratio $I_P/I_0$ as a function of the benzene density for reactions (2) and (5), measured with the GIB-MS set up, is shown in Figures 3a and 3b, respectively. Data have been collected at the lowest collision energy achievable for the present system in our apparatus, about 0.25±0.05 eV in the center of mass frame. We observe a linear dependence up to a density value of about $5\times10^{12}$ molecules·cm$^{-3}$ (corresponding to a benzene pressure of about $2\times10^{-4}$ mbar). By fitting the pressure-dependent data, the absolute values of the reactive cross section $\sigma_P$ can be estimated, as detailed in Section 2. The $\sigma_P$ values for channels (2) and (5) are 1.0±0.3 Å$^2$ and 2.0±0.6 Å$^2$, respectively. The positive deviation from linearity, *i.e.* the higher product yield observed at higher benzene densities, can be due to several factors. In particular, multiple collisions can cool internal degrees of freedom of the ionic reactants and/or of the intermediate complexes, and at the same time they can collisionally stabilize products. In addition, a multi-collisional regime tends to thermalize the reactant kinetic energy.

Absolute cross section values can be converted into phenomenological rate constants *k(E')* by using the expression $k(E') = v\cdot\sigma_P(E)$, where *k(E')* is the rate constant in cm$^3$·s$^{-1}$, $\sigma_P$ is the reactive cross section for product channel P in cm$^2$, $v = (2E/\mu)^{1/2}$ is the nominal center of mass velocity in cm·s$^{-1}$, and $\mu$ is the reduced mass of the reactants in kg. The mean relative energy of the reactants is $E' = E + (3/2)\gamma k_B T$, where $\gamma$=M/(M+m) and $T$ is the

neutral gas temperature.[27] By using the above mentioned experimental data for the reactive cross sections and the branching ratios reported in Table 1, column *(a)*, we obtain a total phenomenological rate constant for the reaction $C_{10}H_7^+ + C_6H_6 \rightarrow$ all products, $k = (5.8\pm1.9)\times10^{-11}$ cm$^3$·s$^{-1}$ at $E' \approx 0.27$ eV.

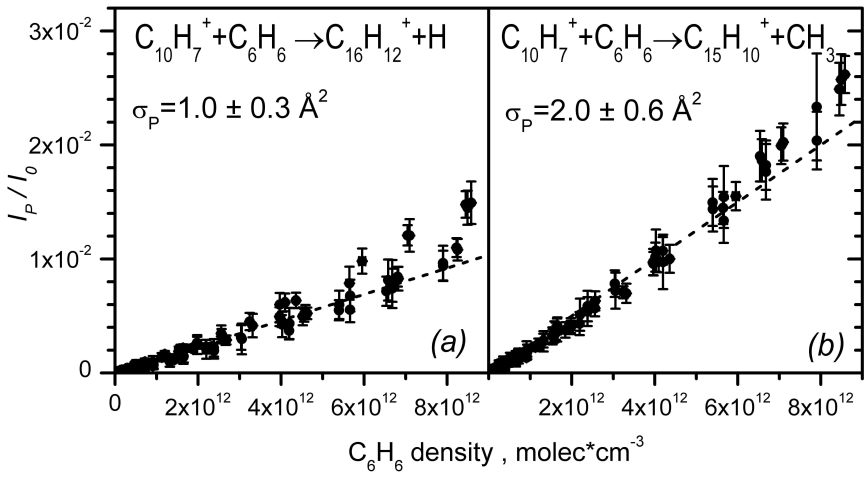


**Figure 3**: Density dependences of: *(a)* $C_{16}H_{12}^+$ and *(b)* $C_{15}H_{10}^+$ products after the reaction of $C_{10}H_7^+$ with $C_6H_6$ at a collision energy of 0.25±0.05 eV in the center of mass frame. Dashed lines are linear fits of the data.

Reactive cross sections for channels (1) - (8) have been measured as a function of the collision energy in the range 0.1-3 eV, by using the GIB set-up, at a benzene pressure of ~ $8\times10^{-5}$ mbar to ensure single collision conditions. For the $C_{16}H_{12}^+$ and $C_{15}H_{10}^+$ products, absolute values of the cross section have been also measured at one specific energy, as already described. Cross sections at the other collision energies and for the other channels have been rescaled accordingly, by using the relative intensities of products. In this way absolute cross sections as a function of collision energy are derived and shown in Figure 4. A common trend is the negative energy dependence of the cross sections, indicating overall exothermic processes, hence possible energy barriers should be lower than the total energy presumably available to the reactants. The cross section for reaction (1) (open squares in Figure 4a) shows the steepest decrease as the collision

energy increases, which fits with a $E_{CM}^{-1.3}$ dependence (shown by the blue line in Figure 4).

Several other channels leading to the loss of neutral fragments (i.e., H, $H_2$, $CH_3$, etc…) can lower the yield of the initial intermediate, thereby explaining the low yield of reaction (1) when carried out at low benzene pressure. The similar energy dependences of all the other channels (2)-(8) suggest that these reactions proceed via a complex-mediated mechanism, *i.e.* by formation and subsequent fragmentation of the association product $C_{10}H_7{\cdot}C_6H_6^+$, with complex formation probability and lifetime strongly suppressed by an increase in the collision energy. We note in passing that the absolute value of the cross section for formation of the benzene addition product from naphthylium ion is smaller than the similar channel leading to $C_{12}H_{11}^+$ from phenylium ion, the latter having a cross section of 1.9±0.5 $Å^2$ at 0.23 eV.[17]

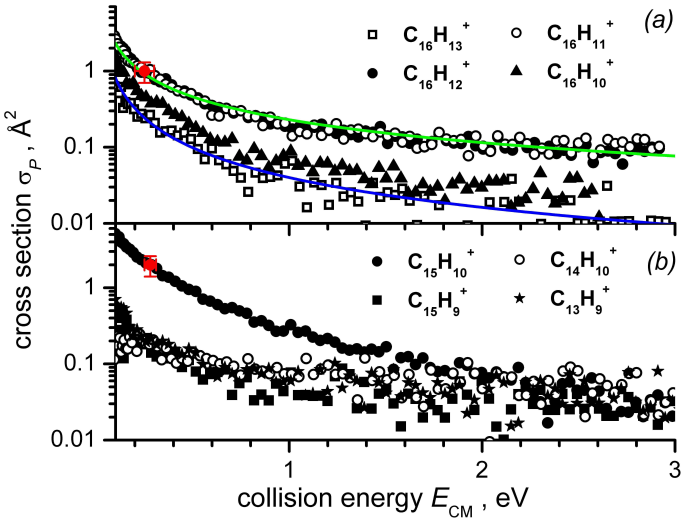


**Figure 4**: Cross sections as a function of the collision energy for the reaction of $C_{10}H_7^+$ with $C_6H_6$ leading to the following products: *(a)* $C_{16}H_n^+$ with n=13-10; *(b)* $C_{15}H_{10}^+$, $C_{15}H_9^+$, $C_{14}H_{10}^+$ and $C_{13}H_9^+$. Red points corresponds to the absolute values of the cross sections for channels (2) and (5), directly obtained from analysis of data shown in Fig. 3. Lines in *(a)* are guide for the eye indicating a dependence $E_{CM}^{-1}$ (green) and $E_{CM}^{-1.3}$ (blue).

To shed more light on the reaction mechanism and on the structure of the adduct complex in the reaction of naphthyl cations with benzene we have performed collision induced dissociation experiments on the cation $C_{16}H_{13}^+$ (*m/z* 205) by using $N_2$ as fragmentation gas. Primary ions at *m/z* 205 are produced in the APCI source by infusion of a solution of commercial phenylnaphthalene in methanol (0.1 mol/liter). The resulting

MS/MS spectrum (reported in Figure 5) shows a fragmentation pattern in which the most intense ionic fragments occur at *m/z* 204 (loss of H), 203 (loss of $H_2$), 202 (loss of $H+H_2$) and 190 (loss of $CH_3$). Thus collision induced dissociation of $C_{16}H_{13}^+$ (having the structure of protonated phenylnaphthalene) affords fragments having the same masses of the ions produced in the reaction of $C_{10}H_7^+$ with benzene (compare MS spectra and peak positions in Figures 2 and 5). Other fragments are detected, although with smaller intensities at *m/z* 178 (formal loss of $C_2H_3$), 165 (formal loss of $C_3H_4$), 149 and 145 plus *m/z* 77 (in very low yield, formal loss of $C_{10}H_8$). It is worth noting that such fragments are detectable only at high collision energies (*i.e.* above 20 eV, nominal in the lab).

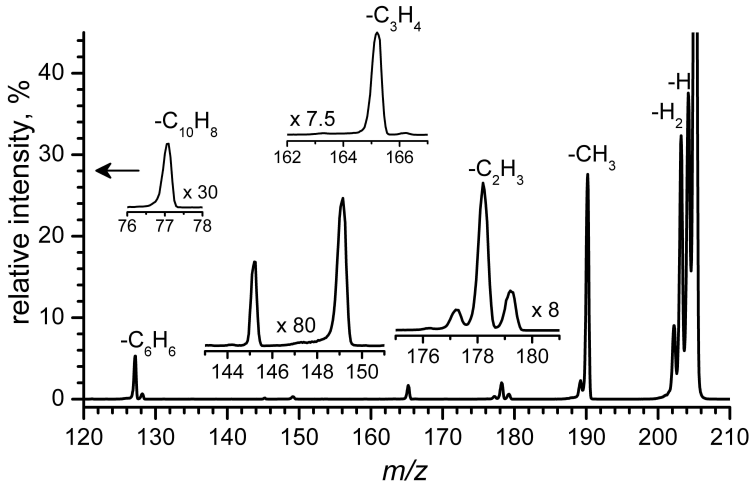


**Figure 5:** MS/MS spectrum of the *m/z* 205 ion generated by infusion of phenylnaphthalene in the APCI source, using $N_2$ as CAD gas at a pressure ~$10^{-3}$ mbar and a nominal collision energy of 28 eV in the LAB.

The MS/MS experiment supports the idea that the reaction of naphthyl cation with benzene proceeds via a long lived intermediate complex, for which we can conjecture the structure of protonated phenylnaphthalene. When the internal energy content is high enough, the complex can dissociate along several channels, the principal ones being the loss of light fragments (H, $H_2$, methyl).

The reactivity of naphthylium ions with benzene molecules has been investigated in previous radiolytic studies carried out using both gaseous benzene (at pressures in the range 7-80 mbar, *i.e.* much higher than those used in present experiments) and liquid benzene.[28, 29] The main observed products, after neutralization via proton transfer with the substrate or the reactor walls, are 1- and 2- phenylnaphthalenes as well as fluoranthene

$C_{16}H_{10}$, observed only in one case and in rather low yield.[28] We underline the fact that a quantitative comparison between our and previous experiments is not straightforward due to the different pressure regimes used (single or close to single collision in our case and strongly multi-collisional regime in refs. 28 and 29). However we note that the overall C-C coupling reactions having small reactive cross sections in our low-pressure experiments, occur with rather high overall absolute yields (up to 46%) at elevated benzene pressures.[29]

### 4.2 Theoretical results and reaction mechanisms

One of the more prominent peaks in Figure 1 is relevant to the $C_{15}H_{10}^{+}$ radical cation, which can form upon methyl radical loss from $C_{16}H_{13}^{+}$ (reaction 5). Since its origin does not appear obvious, the purpose of this theoretical part of the study is to focus on the possible transformations leading to it. First, naphthylium can be generated with two accessibile spin multiplicities, singlet and triplet.[30] Since they are separated by only 3 kcal·mol$^{-1}$, in favour of the singlet,[31] they can be deemed accessible both, under present experimental conditions. However, upon exploration of the first reaction steps for the triplet, sizeable barriers have been assessed, that discouraged a full study. Therefore, the energies so defined are just reported in note for completeness,[32] making reference, as regards structure identification, to the same numbers used for the singlet (see Scheme 1). The results obtained on the singlet hypersurface are presented in the following, discussing CBS $\Delta E_{ZPE}$ values, while geometries and energies can be found in the EPAPS file.[33] The singlet pathways can be considered reasonably to be at the origin of the largest part of the observed products.

Naphthylium acts as an electrophile and adds to the $\pi$ system of benzene, leading initially to the formation of an ionic adduct with an exothermicity of about 53 kcal·mol$^{-1}$ (*i.e.* lying at –53 kcal·mol$^{-1}$ with respect to the reagents, taken as our reference energy throughout). Starting from structure **1** several rearrangements have been explored, apt in

principle to lead to a methyl radical loss. We have found that the only sequences of events suitable to get in the end a methyl loss include: (1) a ring closure leaving a methylenic group connecting two other carbons, $C_a$ and $C_b$ in Scheme 1 and 4 (which can be bridgeheads or not); (2) cleavage of one of the two bonds $C_a$–C or C–$C_b$ in the bridge $C_a$—$CH_2$—$C_b$, to get an exocyclic methylenic group; (3) a final H shift to generate the methyl group, which then dissociates. One or more H shifts can occur in between the above stages. Steps 2 and 3 may be concerted. Consequently, only the most promising pathways are displayed in Schemes 1- 4 and their key passages are illustrated in the following.

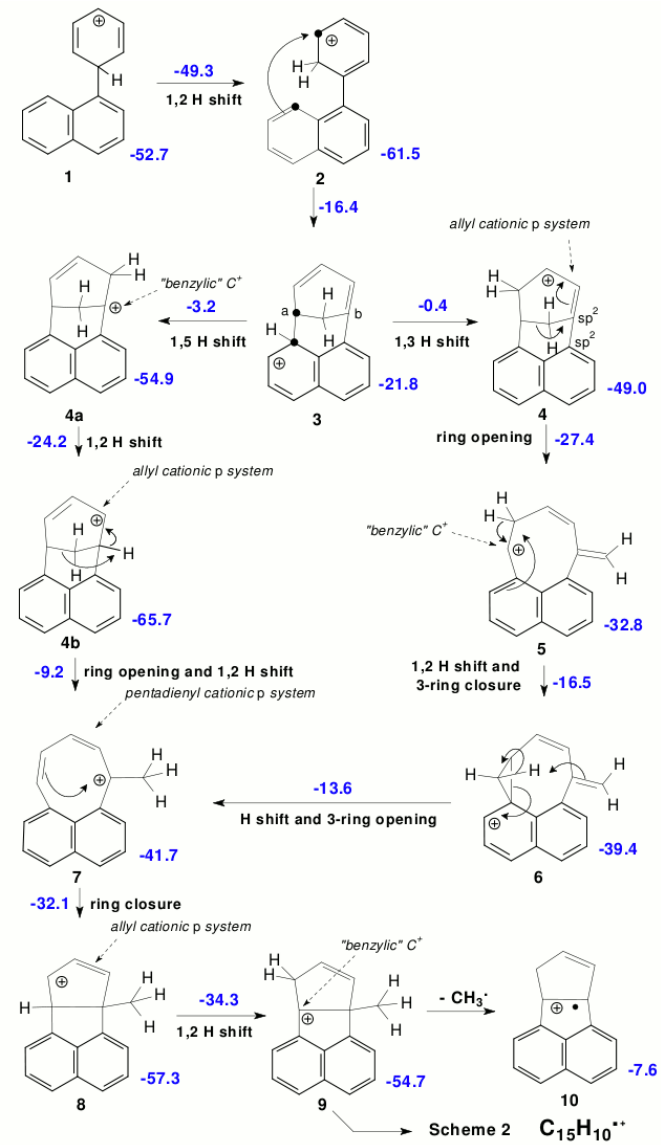


**Scheme 1:** Structures and energies of the most relevant stationary points on the reactive potential energy surface leading from $C_{10}H_7^+$ plus benzene to $C_{15}H_{10}^{\cdot+}$ (structure **10**) plus $CH_3$. Hydrogen atoms are explicitly indicated when they are involved in shifts or gradual $CH_3$ formation. Energies are in kcal·mol$^{-1}$.

On the onset, after an easy 1,2 H transfer, the key step for the subsequent formation of a methyl group is the electrophilic addition **2**-**3**, whose barrier is at –16 kcal·mol$^{-1}$ with respect to the reagents (see Scheme 1). It brings about the formation in **3** of a bicyclic subunit condensed with the rings formerly belonging to naphthylium (n-rings), located in turn at –22 kcal·mol$^{-1}$ with respect to the reagents. This subunit carries a methylenic group as a one-carbon bridge, indicated as $C_a$—$CH_2$—$C_b$ in Schemes 1 and 4, which is the future nucleus for methyl group formation. This rearrangement has an energetic cost which can easily be sustained by the evolving system. Then, two alternative H transfers (**3**-**4** and **3**-**4a**) can restore the aromaticity of the leftmost n-ring.

However the H shifts require overcoming sizable energy barriers, which bring the system energy close to the zero defined by the separate reactants. **3**-**4a** is slightly favoured, having a barrier at –3 kcal·mol$^{-1}$ with respect to the reagents. Then, the energy gain so attained is not negligible, since the energy of the system is now comparable in both cases to that of the initial adduct (**4a**: –55 kcal·mol$^{-1}$; **4**: –49 kcal·mol$^{-1}$). From **4**, ring opening and further H shifts produce first an 8-membered ring that carries a methyl substituent, **5**, –33 kcal·mol$^{-1}$, followed by two H shifts to get **7**, at –42 kcal·mol$^{-1}$. Both barriers relevant to these steps are well below our reference energy. The isomer **7** can be obtained also from **4a** and then **4b**, through an H shift and subsequent ring opening (with barriers at –24 and –9 kcal·mol$^{-1}$). So, both pathways stemming from **3**, finally converge on **7**. Then a final ring closure with formation of two condensed 5-membered rings leads from **7** to **8** (at –57 kcal·mol$^{-1}$). Another H shift and a final methyl radical loss from **9** (which is at –55 kcal·mol$^{-1}$) lead to the $C_{15}H_{10}^{\cdot+}$ product (**10**). The dissociation limit is at –8 kcal·mol$^{-1}$ with respect to the reagents.

From **9**, an alternative pathway (described in Scheme 2) leads to an isomer of **10**. The first step is a 5-ring opening/4-ring closure (barrier at –36 kcal·mol$^{-1}$ with respect to the

reagents) which forms the spiro intermediate **11**, at –42 kcal·mol$^{-1}$. Its evolution is energy demanding, yet with a barrier still below the reference. A difficult H shift (barrier at –1 kcal·mol$^{-1}$) and a subsequent easier C shift (barrier at –9 kcal mol$^{-1}$) generate an intermediate in which the migrating C (highlighted with a green dot in Scheme 2) brigdes onto two carbons of one n-ring (**13**, at –31 kcal·mol$^{-1}$). Then the 3-membered ring breaks and a ring expansion follows (barrier at –19 kcal·mol$^{-1}$), generating a structure resembling phenanthrene, **14**. It is quite stable, at –61 kcal·mol$^{-1}$. A further H shift allows to create a biphenyl-type structure, and the intermediate **15** is even more stable (–77 kcal·mol$^{-1}$). The dissociation of a methyl radical leaves the intermediate product **16**, of formula $C_{15}H_{10}^{\cdot+}$. This last step is very endoergic, yet the energy of the dissociation limit is still below the reference by 3 kcal·mol$^{-1}$.

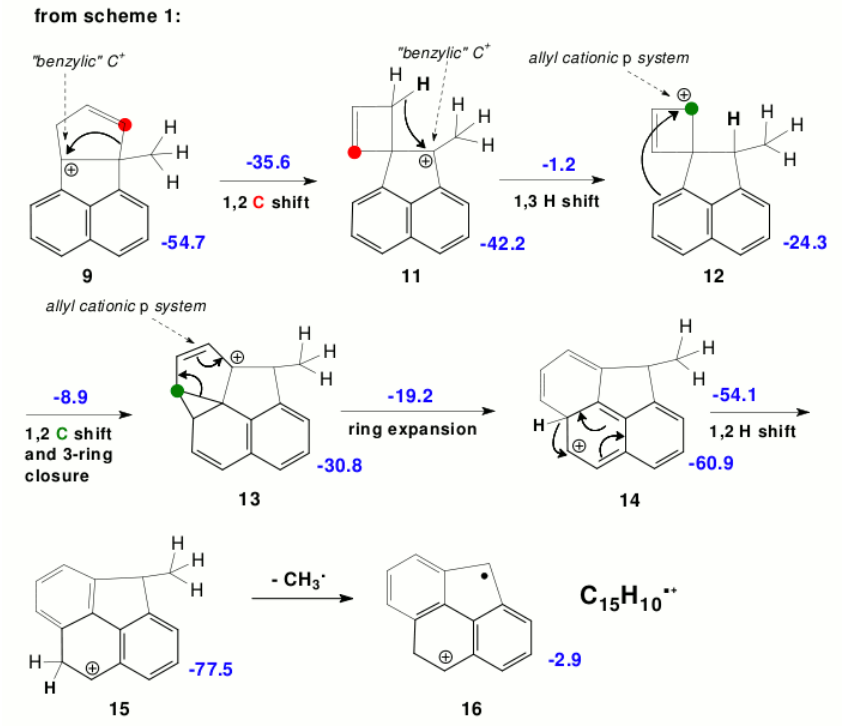


**Scheme 2:** The alternative pathway leading to methyl loss from $C_{16}H_{13}^{+}$ (structure **9**) with formation of $C_{15}H_{10}^{+}$ in an isomeric structure with respect to **10** (described in Scheme 1). Hydrogen atoms are explicitly indicated when they are involved in shifts or gradual $CH_3$ formation. Carbon atoms involved in bond breaking/bond forming steps are highlighted with red and green dots. Energies are in kcal·mol$^{-1}$.

In conclusion, the channel through **3** and **4a** implies overcoming a slightly lower barrier than that through **3** and **4**. Then the step from **9** to **10** with methyl loss goes up to -8 kcal·mol$^{-1}$, while that from **9** to **11** and **12** has to go up to –1 kcal·mol$^{-1}$. All considered, the

description of the $C_{16}H_{13}^+ \rightarrow C_{15}H_{10}^{\cdot+}$ evolutions offered above appears consistent with the height of the $C_{15}H_{10}^{\cdot+}$ peak.

We have also explored the possibility of methyl loss involving a carbon that belongs to one n-ring. Also in this case we describe as an example only a channel presenting lower barriers for methyl loss. For this alternative process to proceed, the **1**-**3** sequence outlined above (see Scheme 1) should actually be preceded by preliminary hydrogen migrations to position 4 of the formerly naphthylium part (**1**$^{IV}$ in Scheme 3), in order to form a methylenic group (in the initial adduct **1** the n-ring is bound to the phenyl part by its position 1). We note in passing that isomers **1**$^{I}$ - **1**$^{IV}$ having the "extra" hydrogen bound to a $sp^3$ carbon belonging to the "naphthalene" part of the adduct, actually have lower energies than **1** itself, the most stable one being structure **1**$^{IV}$ that lies ~21 kcal·mol$^{-1}$ lower than structure **1**.

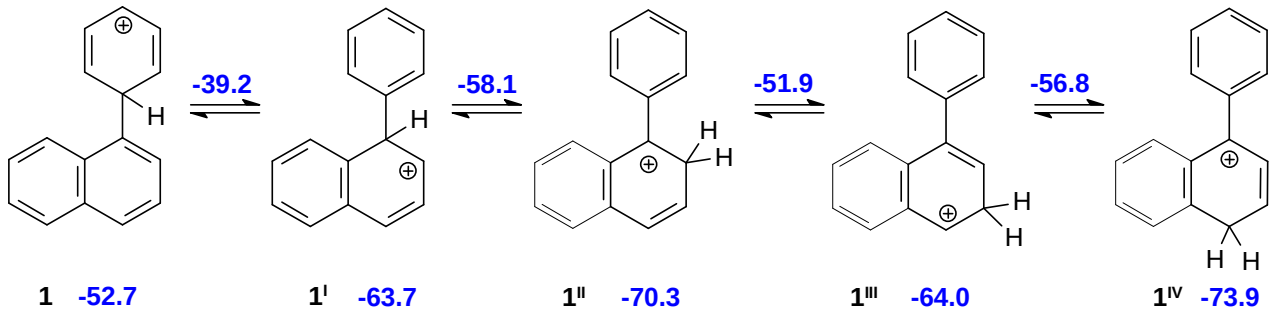


**Scheme 3:** Structures and energies of the hydrogen migrations along the rings of the $C_{16}H_{13}^+$ adduct. Shifting hydrogens are explicitly indicated. Energies are in kcal·mol$^{-1}$.

The complete mechanism for methyl loss from the n-rings is represented in Scheme 4. After H migrations leading to **1**$^{IV}$, the next step entails binding one *ortho* carbon of the phenyl part to the 3 position (which becomes $C_b$) in the rightmost n-ring (the C atoms involved in this step are highlighted by black dots in structures **1**$^{IV}$ and **17** of Scheme 4). The ring closure step brings the reacting system to an higher energy with respect to the reference level defined by the two reactants (structure **17**, at +1.1 kcal·mol$^{-1}$). Then, a bond cleavage involving the $CH_2$ group would follow: two are possible, but only breaking of

$CH_2$–$C_b$ is relatively easy. After some H shifts the methyl group is formed. One ring closure and a few other H shifts and it can leave without attaining too high an energy (+4.2 kcal·mol$^{-1}$ with respect to reagents). Methyl loss from **21**-**24** does not allow to form a biphenyl structure which can be attained only from **25**.

In concluding the survey of the most viable channels it is worth pointing out that the $CH_3$ loss from phenyl (Schemes 1 and 2) is at any step below the reference level defined by reagents, and thus is a viable pathway for methyl loss in cold environments such as the interstellar medium or Titan's ionosphere.

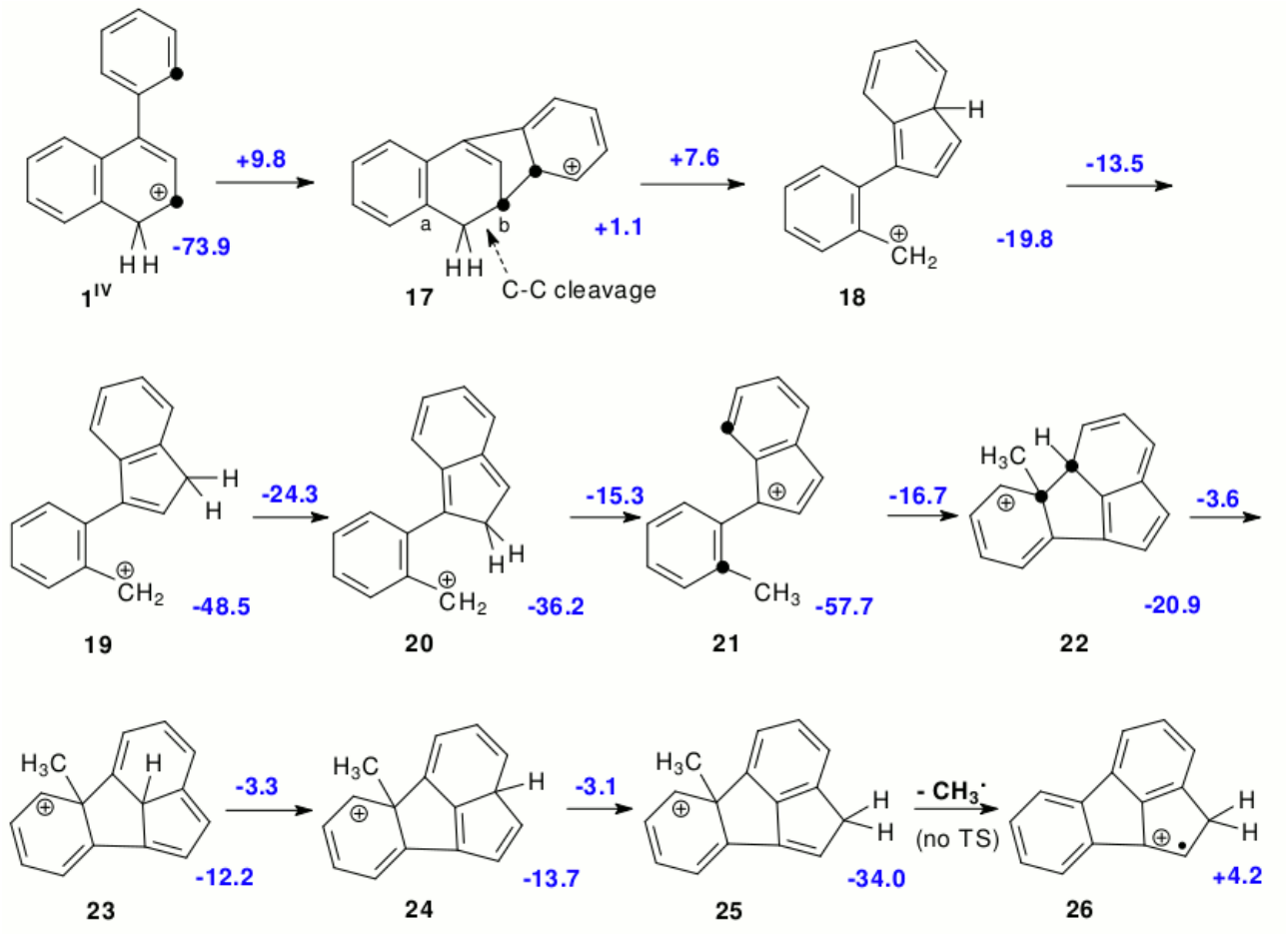


**Scheme 4:** The alternative pathway leading to methyl loss from the naphthylium moiety. Hydrogen atoms are explicitly indicated when they are involved in shifts or gradual $CH_3$ formation. Energies are in kcal·mol$^{-1}$.

Regarding the formation of $C_{16}H_{12}^+$ and $C_{16}H_{11}^+$, we expect that the high exothermicity of reaction (1) leading to structure **1** favours further chemical rearrangements giving rise to H and $H_2$ losses, reactions (2)-(4), maybe as a consequence of self-condensation reactions resulting in fluoranthene-like structures, as put forward in Ref. 28. However the theoretical investigation of these reactive channels is beyond the scope of the present paper.

### 4.3 H/D scrambling

Further measurements have been carried out in the APCI-TQ-MS by using isotopically labelled $C_6D_6$ as neutral reagent, with the purpose of investigating any possible H/D atom scrambling during reactions (2)-(9) and of observing channels leading to back-fragmentation of the association product adduct into reactants. A typical mass spectrum of products from the reaction of $C_{10}H_7^+$ (produced in the APCI source) with $C_6D_6$ taken at a collision energy $E_{CM}$ ~ 0.5-1 eV and benzene-$d_6$ pressure ~ $9.5\times10^{-4}$ mbar is shown in Figure 6. The mass spectrum is complicated by extensive H/D atom scrambling in some of the reaction products, similar to what previously observed in the phenyl cation/benzene system.[17]

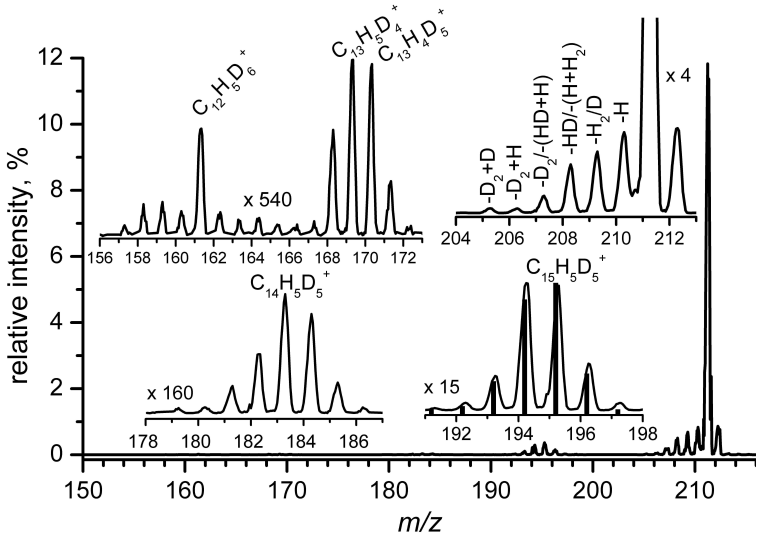


**Figure 6:** MS spectrum of ionic products from the reaction of mass-selected $C_{10}H_7^+$ ions with $C_6D_6$ recorded in the APCI-TQ-MS set up at a collision energy $E_{CM}$ ~ 1 eV in the CM frame (3.6 eV in the LAB) and with ~$9.5\times10^{-4}$ mbar of benzene-$d_6$ in the reaction cell. Vertical bars represents the calculated intensities corresponding to a complete randomization of position of H and D atoms in the ion $C_{15}(H,D)_{10}^+$ formed according to reaction (5).

In ion-molecule reactions leading to arenium-like ions (e.g. protonated benzene, protonated naphthalene and protonated biphenyl)[17,34,35] H/D atom scrambling implies a reactive mechanism that proceeds via the formation of an intermediate complex, whose lifetime is long enough to allow a redistribution of the H and D atoms over the rings via 1,2-hydrogen shift, both intra and inter rings (the benzyl and naphthyl rings in the present case of $C_{16}H_{13}^+$ having the structure of protonated phenylnaphthalene). The reactive channel that is most easily reanalyzed in terms of H/D scrambling is reaction (5), leading to $C_{15}H_{10}^+$ at *m/z* 190 in the case of benzene-$h_6$. In Figure 2 two peaks at *m/z* 189 and 191 are visible but with much smaller intensity compared to *m/z* 190: peak at *m/z* 189 corresponds to production of $C_{15}H_9^+$, with an intensity about 14 times lower than $C_{15}H_{10}^+$, while the contribution of $C_{15}H_{11}^+$ to the peak at *m/z* 191, when $^{13}C$ contribution is taken into account, is over a factor 90 smaller than $C_{15}H_{10}^+$. When naphthyl cations are reacted with benzene-$d_6$ a cluster of ions is observed in the *m/z* region 192-198, with the highest intensity at the mass of $C_{15}H_5D_5^+$ (*m/z* 195). The relative intensities of the peaks 193-196 within the cluster can be calculated assuming a *complete randomization* of the 7 H and 6 D atoms over both benzyl and naphthyl ring systems at the level of the intermediates $C_{16}H_7D_6^+$ (indicated as **1** and **2** in Scheme 1 and $\mathbf{1^I}$ - $\mathbf{1^{IV}}$ in Scheme 3) prior to production of $C_{15}(H,D)_{10}^+$ and, though in smaller amounts, of $C_{15}(H,D)_9^+$ and $C_{15}(H,D)_{11}^+$. From an energetic point of view H atoms can freely “walk” along both rings since barriers for 1,2 H shifts always lie well below the reactant energy. Peak intensities expected for complete statistical scrambling can be calculated by making allowance for the presence of $^{13}C$ at natural abundance in the $C_6D_6$ reacting partner,[36] and taking into account the presence of channels leading to $C_{15}(H,D)_9^+$ and $C_{15}(H,D)_{11}^+$, as well as $C_{15}(H,D)_{10}^+$. According to the results obtained in the fully hydrogenated case, the relative intensities of the three channels are in the ratio $C_{15}H_9^+$: $C_{15}H_{10}^+$:$C_{15}H_{11}^+$ = 6.6 : 92.4 : 1.0 and this same ratio is assumed also in the mixed isotope experiment.

The calculated intensities are shown as hatched bars in Figure 7 and are compared with the experimental results (black bars) given in terms of areas of the experimental peaks in the mass range 191-199. Both data have been renormalized to give a total intensity of 100.0. Experimental intensities are in good, though non perfect agreement, with calculations from model a), suggesting that the mechanism for formation of $C_{15}(H,D)_n^+$ (with n=9-11) ions involves a high degree of H/D randomization over both the naphthyl and phenyl rings.

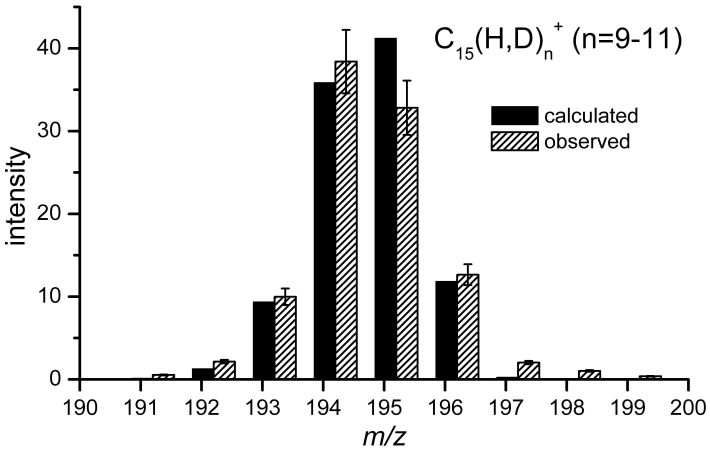


**Figure 7:** Experimental intensities of products from the reaction of $C_{10}H_7^+$ with $C_6D_6$ are compared with calculations assuming a complete randomization of the H and D atoms in the $C_{16}H_7D_6^+$ complex prior to dissociation leading mainly to $C(H,D)_3$ loss.

## 5. Conclusions

PAHs are ubiquitous molecules that are found in very different environments and understanding their formation is a topic of current research. In the present work we have explored mechanisms for the molecular growth based on ion-molecule reactions, which can be relevant in ionized gases such as planetary ionospheres, plasmas and combustion systems. The reaction of naphthyl cation $C_{10}H_7^+$ with benzene has been investigated by using tandem mass spectrometers and reactive cross sections have been measured as a function of the collision energy. We have detected the association product $C_{16}H_{13}^+$ and various lighter cations corresponding to the loss of H, $H_2$, $CH_3$.

Experiments performed by using isotopic reagents indicate an almost statistical scrambling of H,D atoms among the different rings, thus suggesting that the reaction

proceeds via a long lived association product, presumably the covalently bound protonated phenylnaphthalene, from which lighter species are generated by elimination of neutral fragments. In particular the reaction channel $C_{10}H_7^+ + C_6H_6 \rightarrow C_{15}H_{10}^{\cdot+} + CH_3$ has been theoretically investigated by DFT calculations, and at least two exoergic mechanisms have been found (sketched in Scheme 1 and Scheme 2). This result is a clear example for the possibility of molecular growth via ion-molecule reactions, and may be relevant for explaining the detection of large PAHs in diverse environments, in those cases when a certain degree of molecular ionization is present.

**Acknowledgements**

The authors wish to thank Damiano Avi for skilled technical support during the experiments. This work was conducted in the frame of EC FP6 NoE ACCENT (Atmospheric Composition Change, the European NeTwork of Excellence). Support from the University of Trento is gratefully acknowledged.

## References


[1] S. Iglesias-Groth, A. Manchado, D.A. Garcia-Hernandez, J.I. Gonzalez Hernandez, D.L. Lambert, Astrophys. J. **685**, L55-L58 (2008).

[2] C.S. McEnally, L.D. Pfefferle, B. Atakan, K. Kohse-Höinghaus, Prog. Ener. Combust. Science **32** 247 (2006).

[3] A.N. Eraslan, R.C. Brown, Combust. Flame **74**, 19 (1988).

[4] A.M. Starik, A.M. Savel'ev, N.S. Titova, Plasma Source Sci. Technol. **17**, 045012 (2008).

[5] H. Haverkamp, S. Wilhelm, A. Sorokin, F. Arnold, Atmosph. Environment **38**, 2879 (2004).

[6] D.K. Bohme, S. Wlodek, J.A. Zimmerman, J.R. Eyler, Int. J. Mass Spectrom. Ion Proc. **109**, 31 (1991).

[7] P.O. Momoh, S.A. Abrash, R. Mabourki, M.S. El-Shall, J. Am. Chem. Soc. **128**, 12408 (2006).

[8] P.O. Momoh, A.-R. Soliman, M. Meot-Ner, A. Ricca, M.S. El-Shall, J. Am. Chem. Soc. **130**, 12848 (2008).

[9] M.S. El-Shall, Y. M. Ibrahim, E. H. Alsharaeh, M. Meot-ner (Mautner), S. P. Watson, J. Am. Chem. Soc. **131**, 10066 (2009).

[10] C.L. Ricketts, D. Schroder, C. Alcaraz, J. Roithova, Chem. Eur. J. **14**, 4779 (2008).

[11] J.H. Waite , D.T. Young, T.E. Cravens, A.J. Coates, F.J. Crary, B.A. Magee, J. Westlake, Science **316**, 870 (2007).

[12] J.-E. Wahlund, M. Galand, I. Müller-Wodarg, J. Cui, R.V. Yelle, F.J. Crary, K. Mandt, B. Magee, J.H. Waite Jr., D.T. Young, A.J. Coates, P. Garnier, K. Agren, M. Andre, A.I. Eriksson, T.E. Cravens, V. Vuitton, D.A. Gurnett, and W.S. Kurth, Plan. Space Sci. **57**, 1857 (2009).

[13] F.J. Crary, B.A. Magee, K. Mandt, J.H. Waite Jr., J. Westlake, and D.T. Young, Plan. Space Sci. **57**, 1847 (2009).

[14] E.C. Sittler Jr., A. Ali, J.F. Cooper, R.E. Hartle, R.E. Johnson, A.J. Coates, and D.T. Young, Plan. Space Sci. **57**, 1547 (2009).

[15] M.L. Delitsky, and C.P. McKay, Icarus **207**, 477 (2010).

[16] I.P. Robertson, T.E. Cravens, J.H. Waite Jr., R.V. Yelle, V. Vuitton, A.J. Coates, J.E. Wahlund, K. Agren, K. Mandt, B.A. Magee, M.S. Richard, and E. Fatting, Plan. Space Sci. **57**, 1834 (2009).

[17] D. Ascenzi, N. Cont, G. Guella, P. Franceschi, and P. Tosi, J. Phys. Chem. A **111**, 12513 (2007).

[18] A. Giordana, G. Ghigo, G. Tonachini, D. Ascenzi, P. Tosi, and G. Guella, J. Chem. Phys. **131**, 024304 (2009).

[19] P. Tosi, G. Fontana, S. Longano, and D. Bassi, Int. J. Mass Spectrom. Ion Proc. **93**, 95 (1989).

[20] P. Franceschi, L. Penasa, D. Ascenzi, D. Bassi, M. Scotoni, and P. Tosi, Int. J. Mass Spectrom. **265**, 224 (2007).

[21] J. A. Pople, P. M. W. Gill, B. G. Johnson, Chem. Phys. Lett. **199**, 557 (1992); H. B. Schlegel, in *Computational Theoretical Organic Chemistry*, edited by I. G. Csizsmadia and R. Daudel (Reidel Publishing Co., Dordrecht, The Netherlands, 1981), p. 129-159; H. B. Schlegel, J. Chem. Phys. **77**, 3676 (1982); H. B. Schlegel, J. S. Binkley, and J. A. Pople, *ibid.* **80**, 1976 (1984); H. B. Schlegel, J. Comput. Chem. **3**, 214 (1982).

[22] R. G. Parr, W. Yang, *Density Functional Theory of Atoms and Molecules* (Oxford University Press, New York, 1989), Chapt. 3.

[23] Y. Zhao and D. G. Truhlar, Theor. Chem. Acc. **120**, 215 (2008); Y. Zhao and D. G. Truhlar, Acc. Chem. Res. **41**, 157 (2008); Y. Zhao and D. G. Truhlar, J. Phys. Chem. A **112**, 1095 (2008); Y. Zhao and D. G. Truhlar, J. Chem. Theory & Comput. **4**, 1849 (2008).

[24] E. Woon and T. H. Dunning Jr., J. Chem. Phys. **98**, 1358 (1993).

[25] A. Halkier, T. Hegaker, P. Jørgensen, W. Klopper, H. Koch, J. Olsen, A.K. Wilson, Chem. Phys. Lett. **286**, 243 (1998).

[26] Gaussian 09, Revision A.02, M. J. Frisch, G. W. Trucks, H. B. Schlegel, G. E. Scuseria, M. A. Robb, J. R. Cheeseman, G. Scalmani, V. Barone, B. Mennucci, G. A. Petersson, H. Nakatsuji, M. Caricato, X. Li, H. P. Hratchian, A. F. Izmaylov, J. Bloino, G. Zheng, J. L. Sonnenberg, M. Hada, M. Ehara, K. Toyota, R. Fukuda, J. Hasegawa, M. Ishida, T. Nakajima, Y. Honda, O. Kitao, H. Nakai, T. Vreven, J. A. Montgomery, Jr., J. E. Peralta, F. Ogliaro, M. Bearpark, J. J. Heyd, E. Brothers, K. N. Kudin, V. N. Staroverov, R. Kobayashi, J. Normand, K. Raghavachari, A. Rendell, J. C. Burant, S. S. Iyengar, J. Tomasi, M. Cossi, N. Rega, J. M. Millam, M. Klene, J. E. Knox, J. B. Cross, V. Bakken, C. Adamo, J. Jaramillo, R. Gomperts, R. E. Stratmann, O. Yazyev, A. J. Austin, R. Cammi, C. Pomelli, J. W. Ochterski, R. L. Martin, K. Morokuma, V. G. Zakrzewski, G. A. Voth, P. Salvador, J. J. Dannenberg, S. Dapprich, A. D. Daniels, Ö. Farkas, J. B. Foresman, J. V. Ortiz, J. Cioslowski, and D. J. Fox, Gaussian, Inc., Wallingford CT, 2009.

[27] P. Tosi, Chem Rev. **92**, 1667 (1992).

[28] G . Angelini, Y. Keheyan, E . Lilla, G. Perez, Radiochim. Acta **51**, 173 (1990).

[29] Y. Keheyan, R. Bassanelli, Radiat. Phys. Chem. **47**, 465 (1996).

[30] M. Slegt, F. Minne, H. Zuilhof, H.S. Overkleeft, and G. Lodder, Eur. J. Org. Chem. **32**, 5353 (2007).

[31] We can report that in ref. 30 the reverse ordering was found: “calculations at the B3LYP/6-311G(d,p) in vacuo give the triplet as the most stable structure, with the singlet lying only 1.1 kcal·mol$^{-1}$ higher in energy”.

[32] We report here some cc-pvTZ energy differences. Starting from naphthylium in the triplet state, **1** is at -28.3 kcal·mol$^{-1}$ and the barrier for H migration (**1**-**2**) is +6.3 kcal·mol$^{-1}$ above the reactants. The C-C bond formation (**2**-**3**) from **2** (-32.9 kcal·mol$^{-1}$) is located at +7.9 kcal·mol$^{-1}$ and leads to

the intermediate **3** (-2.5 kcal·mol$^{-1}$ with respect to the reactants). Both H migrations form **3** (**3**-**4a** and **3**-**4**) have energy barriers above the reactants: +25.6 and +13.8 kcal·mol$^{-1}$ respectively.

[33] See Supplementary Material Document No._____ for M06-2X/CBS // M06-2X/cc-pvTZ optimized structures of reactants, products, transition structures and intermediates: energies, and Cartesian coordinates. For information on Supplementary Material, see http://www.aip.org/pubservs/epaps.html.

[34] D. Ascenzi, D. Bassi, P. Franceschi, P. Tosi, M. Di Stefano, M. Rosi, and A. Sgamellotti, J. Chem. Phys. **119**, 8366 (2003).

[35] D. Ascenzi, D. Bassi, P. Franceschi, O. Hadjar, P. Tosi, M. Di Stefano, M. Rosi, and A. Sgamellotti, J. Chem. Phys. **121**, 6728 (2004).

[36] $^{13}C$ contributions of peaks at *m/z* = m on peaks at *m/z* = m+1 in the clusters corresponding to $C_{15}(H, D)_n^+$ (n=9-11) amounts to 5.35%.